

# Cyclooctatetraenes Tetrakis-Annulated with $\alpha$ -Dithio- or $\alpha$ -Diselenocarbonyl Groups: Diradicals Predicted To Have Ground States with 10 $\pi$ Electrons in the Eight-Membered Ring and Two-Center, Three-Electron, $\sigma$ Bonds between Two Pairs of Chalcogen Atoms

Xin Zhou, David A. Hrovat, and Weston Thatcher Borden\*

Department of Chemistry and the Center for Advanced, Scientific Computing and Modeling, University of North Texas, 1155 Union Circle, #305070, Denton, Texas 76203-5070

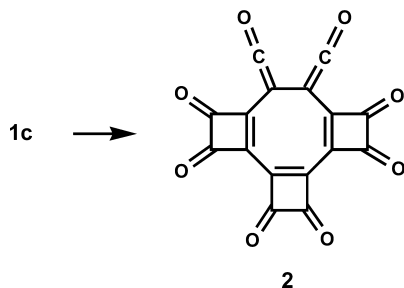
Received: December 10, 2009

(U)B3LYP calculations with the 6-31+G(d) and 6-311+G(2df) basis sets have been carried out on cyclooctatetraenes **6** and **7**, in which the COT ring is tetrakis-annulated with  $\alpha$ -dithio- or  $\alpha$ -diselenocarbonyl groups. Transferring two electrons from the high-lying  $b_{1g}$  and  $e_u$   $\sigma$  MOs in **6** and **7** into the unoccupied, nonbonding, COT  $\pi$  orbital is computed to be energetically favorable. The lowest  $D_{4h}$  electronic state is calculated to be  ${}^3E_u$ , which formally contains 10  $\pi$  electrons in the eight-membered ring and has two unpaired electrons in  $\sigma$  MOs. The  ${}^3E_u$  state undergoes a first-order Jahn–Teller distortion to form **6d** and **7d**, in which the pair of one-electron holes in the  $\sigma$  MOs is stabilized by the formation of two, two-center, three-electron bonds between pairs of chalcogen atoms that are diagonally across the eight-membered ring from each other. The corresponding open-shell singlets are computed to be about 1 kcal/mol lower in energy than the Jahn–Teller distorted triplets. Molecules **6i** and **7i**, in which the C–C bond in one four-membered ring is cleaved, are computed to be lower in energy than **6d** and **7d**. However, a substantial barrier is predicted to separate each of the two pairs of isomers so that **6d** and **7d** should, at least in principle, be isolable.

## Introduction

We have recently reported the results of (U)B3LYP/6-311+G(2df) calculations that found tetrakis-annulated cyclooctatetraene (COT) **1** in Figure 1 has a very low-lying triplet excited state.<sup>1</sup> The planar  ${}^3A_{2u}$  state (**1b**) differs from the lowest singlet state (**1a**) by excitation of an electron from the high-lying,  $b_{1g}$  combination of lone pair orbitals on the oxygens of the cyclobutanedione carbonyl groups<sup>2</sup> into the empty, nonbonding,  $\pi$  MO of the planar COT ring.

Only 6.1 kcal/mol above **1a** in energy is another singlet state (**1c**), in which both electrons that occupy the high-lying  $b_{1g}$   $\sigma$  orbital in **1a** are excited into the empty, nonbonding  $\pi$  MO.<sup>1</sup> However, **1c** is of purely academic interest, because it is computed to break symmetry and undergo a nearly barrierless and highly exothermic opening of one four-membered ring to form bis-ketene **2**, which also has 10  $\pi$  electrons.



Nevertheless, the relatively small energy difference between **1a** and **1c** motivated us to try to identify an analog of **1** that would be calculated to have a singlet ground state with an aromatic dectet of 10  $\pi$  electrons in the COT ring and which

might be stable toward bis-ketene formation. We have found that substituting sulfur or selenium atoms for the oxygens in **1** is, indeed, calculated to result in molecules with ground states containing 10  $\pi$  electrons in the COT ring. However, to our surprise, the lowest electronic state of both the sulfur and selenium analogues of **1** is predicted to be a singlet diradical, with one electron in each of two nearly degenerate  $\sigma$  MOs. Herein, we provide a detailed description of the results of our calculations on the sulfur and selenium analogs of **1**.

**Computational Methodology.** Calculations based on density functional theory were carried out with the three-parameter functional of Becke<sup>3</sup> and the correlation functional of Lee, Yang, and Parr<sup>4</sup> (B3LYP). Geometries were optimized at the unrestricted (U)B3LYP level of theory, and (U)B3LYP vibrational analyses were performed at each stationary point to confirm its identity as a minimum or a transition state. The vibrational frequencies were used, without scaling, to make zero-point corrections to the relative energies. The (U)B3LYP geometry optimizations and vibrational analyses were performed with the 6-31+G(d)<sup>5</sup> basis set, and single-point (U)B3LYP calculations were carried out with the 6-311+G(2df) basis set.<sup>6</sup> These calculations were performed with the Gaussian 03 suite of programs.<sup>7</sup>

To confirm that the singlet diradical ground state, predicted for the sulfur (**6**) and selenium (**7**) analogs of **1**, is not an artifact of the UB3LYP calculations, we also carried out ab initio (2/2)CASSCF and CASPT2 calculations<sup>8</sup> with the 6-31G(d) basis set.<sup>9</sup> The active space consisted of the symmetric and antisymmetric combinations of the singly occupied  $\sigma$  orbitals, formed from the lone-pair AOs on the heteroatoms of **6** and **7**. The (2/2)CASSCF/6-31G(d) optimized geometries were used for the single-point CASPT2 calculations, which were performed with MOLCAS.<sup>10</sup>

\* Corresponding author. E-mail: borden@unt.edu.

**TABLE 1: Adiabatic Ionization Energies (IEs), Electron Affinities (EAs), and Triplet  $n \rightarrow \pi^*$  Excitation Energies (kcal/mol) for 3–5, Obtained by (U)B3LYP Calculations with the 6-31+G(d) Basis Set<sup>a</sup>**

compound	IE	EA	$n \rightarrow \pi^*$
<b>3</b>	203.0 (200.2)	30.4 (30.5)	41.9 (41.6)
<b>4</b>	194.6 (193.9)	54.7 (54.5)	20.4 (20.4)
<b>5</b>	189.3 (190.1)	58.5 (60.5)	15.2 (14.3)

<sup>a</sup> Single-point energies computed with the 6-311+G(2df) basis set are given in parentheses.

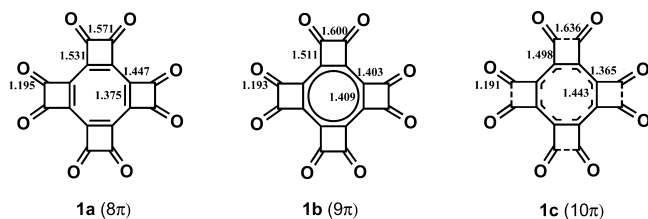
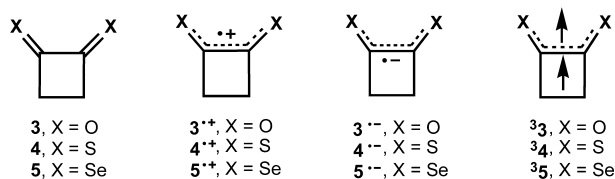


**Figure 1.** Bond lengths (Å) in three low-lying states of tetrakis-annulated COT (**1**).<sup>1</sup> The ground state (**1a**) is a tub-shaped singlet that has eight  $\pi$  electrons in the eight-membered ring. Both the lowest triplet state (**1b**) and the lowest excited singlet state (**1c**) are planar and have, respectively, 9  $\pi$  and 10  $\pi$  electrons in the eight-membered ring. The additional  $\pi$  electrons in the  $^3A_{2u}$  and excited  $^1A_{1g}$  states come from the high-lying  $b_{1g}$  MO,<sup>2</sup> which is doubly occupied in **1a**.

## Results and Discussion

**Calculations on Three Model Compounds.** We began by performing model calculations on cyclobutane-1,2-dione (**3**) and its sulfur (**4**) and selenium (**5**) analogs, to determine the probable effect of substituting sulfur or selenium atoms for the oxygens in **1**. We compared the energies calculated for (a) removing an electron from the highest-lying combination of lone-pair orbitals on the heteroatoms, to form  $3^{3+}-5^{3+}$ , (b) adding an electron to the lowest  $\pi^*$  MO, to form  $3^{3-}-5^{3-}$ , and (c) exciting an electron from the highest-lying combination of lone-pair orbitals on the heteroatoms into the lowest  $\pi^*$  MO, to form the  $n \rightarrow \pi^*$  triplet states ( $^33-^35$ ). A low, lone pair, ionization energy (IE), combined with a high,  $\pi$ , electron affinity (EA), would be expected to result in a molecule with a low  $n \rightarrow \pi^*$  excitation energy. A small  $n \rightarrow \pi^*$  excitation energy is exactly what is required for the sulfur or selenium analogues of **1** to have ground states with 10 instead of 8  $\pi$  electrons.



The results of our calculations of the IEs, EAs, and triplet  $n \rightarrow \pi^*$  excitation energies of **3–5** are given in Table 1. Both the sulfur (**4**) and selenium (**5**) compounds are computed to have substantially lower IEs, substantially higher EAs, and, hence, adiabatic triplet  $n \rightarrow \pi^*$  excitation energies that are, respectively, 21 and 27 kcal/mol lower than that of ketone **3**. Consequently, both octathione **6** and octaselenone **7** in Figure 2 are expected to be better candidates than octaketone **1** in Figure 1 for having a ground state in which two electrons are excited from the highest energy  $\sigma$  MO into the nonbonding COT  $\pi$  MO that is unoccupied in the singlet states (**1a**, **6a**, and **7a**) which have 8  $\pi$  electrons.

**Calculations on 6 and 7 at  $D_{4h}$  Geometries.** The highest occupied (HO)MO of **1a**, **6a**, and **7a** is the  $b_{1g}$  MO, which is shown in Figure 3. It contains the in-phase combination of the lone pair orbitals on the carbonyl groups of each cyclobutane-1,2-dione ring. This combination is destabilized by mixing with the C–C  $\sigma$  bond of the four-membered ring that joins the two carbonyl groups.<sup>1,2</sup> In addition, as shown in Figure 3, in the  $b_{1g}$  MO, the carbonyl lone pair orbitals of each cyclobutane-1,2-dione ring interact in an antibonding fashion with the proximal carbonyl lone pair orbitals in each of the adjacent four-membered rings.

Our B3LYP calculations on **6** and **7** find that at planar,  $D_{4h}$  geometries, the  $^1A_{1g}$  electronic state, with 10  $\pi$  electrons in the COT ring and the  $b_{1g}$   $\sigma$  MO empty (**6c** and **7c**), is lower in energy than either of the  $^1A_{1g}$  states with 8  $\pi$  electrons in the COT ring and the  $b_{1g}$  MO doubly occupied (**6a/b** and **7a/b**). As shown in Table 2, **6c** is computed to be lower in energy than **6a** and **6b** by 16.6 and 18.8 kcal/mol, respectively; and **7c** is computed to be lower in energy than **7a** and **7b** by 23.4 and 21.0 kcal/mol, respectively. Thus, we can predict with some confidence that **6c** and **7c**, each of which has 10  $\pi$  electrons in the COT ring, should be the lowest  $D_{4h}$  singlet state of **6** and **7**, respectively.

We also performed calculations on two triplet states of planar **6** and **7**, in which one electron occupies the  $b_{1g}$   $\sigma$  MO and nine electrons occupy  $\pi$  MOs. The unpaired  $\pi$  electron can occupy either of the two nonbonding, nearly degenerate  $\pi$  MOs of the COT ring. Consequently, there are two low-lying triplet states,  $^3A_{1u}$  and  $^3A_{2u}$ , each with nine  $\pi$  electrons. Table 2 reveals that, at  $D_{4h}$  geometries, these two triplet states are both higher in energy than the 10  $\pi$  electron singlet state (**6c** and **7c**).

There are also two low-lying triplet states with 10  $\pi$  electrons in the COT ring. They differ by which of the three, high-lying,  $\sigma$  MOs in **6** and **7** is occupied by the unpaired electrons and which is occupied by an electron pair. These three  $\sigma$  orbitals (the  $b_{1g}$  MO and a degenerate pair of  $e_u$  MOs) are shown in Figure 3.

The  $b_{1g}$   $\sigma$  MO has one more nodal plane than the degenerate pair of  $e_u$   $\sigma$  MOs, so that the former MO is higher in energy than the latter pair of MOs. Consequently, one would expect that the  $^3A_{2g}$  state, in which the  $b_{1g}$  MO is doubly occupied and each  $e_u$  MO is singly occupied, should be higher in energy than the  $^3E_u$  state, in which only one unpaired electron occupies  $b_{1g}$ , and the other occupies an  $e_u$  MO.

Table 2 confirms that this is, indeed, the case. As also shown by the results in Table 2, the fact that the electrons in the singly occupied  $b_{1g}$  and  $e_u$  MOs in the  $^3E_u$  state have parallel spin leads to this 10  $\pi$  triplet state being computed to be of slightly lower energy than  $^1A_{1g}$ , the 10  $\pi$  singlet state in which the degenerate pair of  $e_u$  MOs is doubly occupied and the  $b_{1g}$  MO is left empty.

**Calculations at Jahn–Teller Distorted Geometries of 6 and 7.**  $^3E_u$ , the  $D_{4h}$  ground state of **6** and **7**, is a degenerate electronic state. Therefore, according to the Jahn–Teller theorem,<sup>11</sup> a distortion from  $D_{4h}$  to lower symmetry must be energetically favorable. Such a distortion further stabilizes  $^3E_u$  relative to  $^1A_{1g}$ , since the latter state is calculated to have a  $D_{4h}$  equilibrium geometry.

One of the Jahn–Teller active vibrations has  $b_{1g}$  symmetry. This vibration shortens the X–X (X = S, Se) distances across the nodal plane in one  $e_u$  MO and lengthens the X–X distances across the nodal plane in the other, thus destabilizing one of these MOs and stabilizing the other. With one of the  $e_u$  MOs in Figure 3 doubly occupied and the other singly occupied, the component of the  $^3E_u$  state that is stabilized has a  $D_{2h}$  geometry

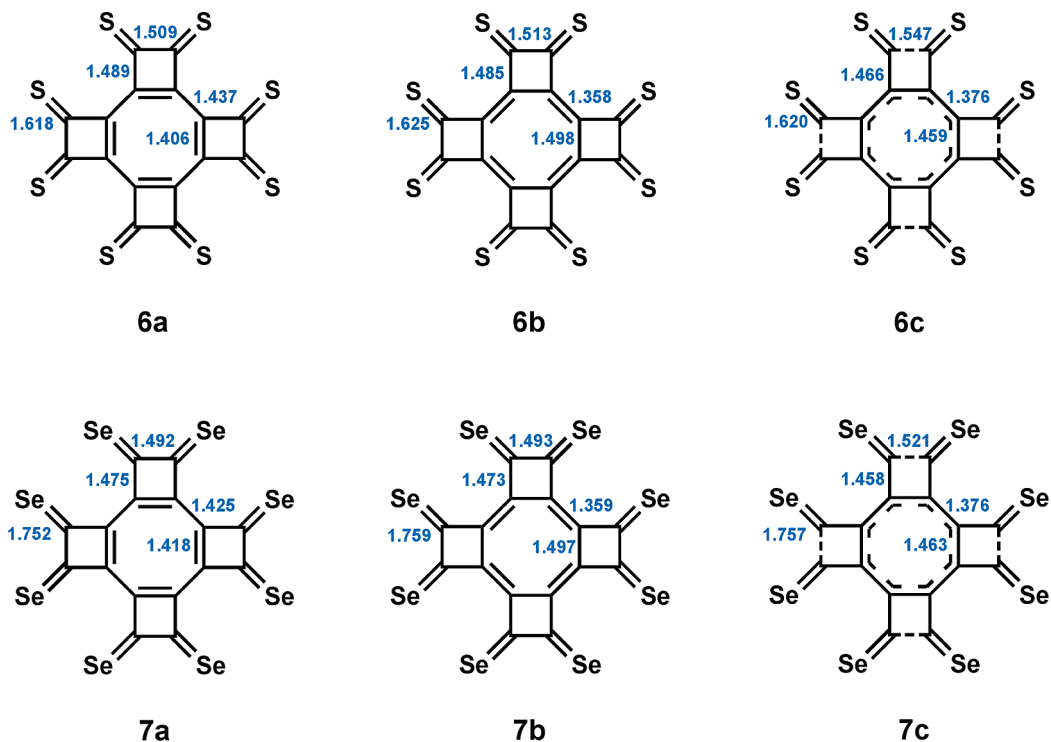


**Figure 2.** Optimized bond lengths in  $D_{2h}$  singlet states of **6** and **7** with 8 (**a** and **b**) and 10  $\pi$  electrons (**c**). The reasons for the longer C–C bonds between the C=X groups in **c** than in **a** or **b** and for the similar bond lengths in the COT rings of **b** and **c** have been previously discussed for the oxygen analog (**1**).<sup>1</sup>

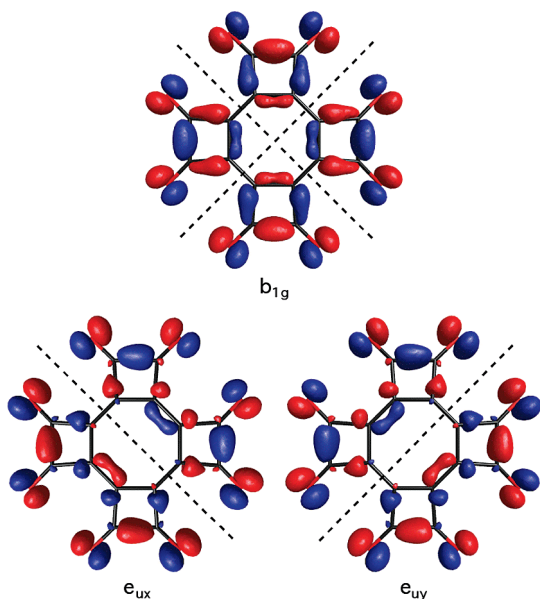


**Figure 3.** The three filled  $\sigma$  MOs of highest energy in **1a**, **6a**, and **7a**. The dotted lines show the locations of the nodes in these MOs.

with a shorter X–X distance across the nodal plane of the singly occupied  $e_u$  MO and a longer X–X distance across the nodal plane of the doubly occupied  $e_u$  MO.

One of the two equivalent, optimized  $D_{2h}$  geometries (**6d** for X = S and **7d** for X = Se) to which the  ${}^3E_u$  state distorts, is shown in Figure 4. At the optimized geometries of **6d** and **7d**, the wave function ( ${}^3B_{3u}$  in  $D_{2h}$  symmetry) puts one unpaired electron in the  $e_{uy}$  MO in Figure 2 and the other in the  $b_{1g}$  MO. Since these two electrons have the same spin, a totally equivalent  ${}^3B_{3u}$  wave function can be written as having one electron in the sum of  $e_{uy}$  and  $b_{1g}$  and the other in the difference of these two MOs.<sup>12</sup>

The sum,  $e_{uy} + b_{1g}$ , localizes one unpaired electron on the lower left-hand side of **6d** and **7d**; and the difference,  $e_{uy} - b_{1g}$ , localizes the other unpaired electron on the upper right-hand side. Therefore, at one of the two equivalent  $D_{2h}$  equilibrium geometries for  ${}^3B_{3u}$ , **6d** and **7d** can each be accurately depicted as shown in Figure 4, with two-center, three-electron bonds<sup>13</sup> formed between pairs of chalcogen atoms that are located diagonally across the eight-membered ring from each other.

The calculated spin densities do, indeed, show half an unpaired electron at each of the four chalcogen atoms involved in two-center, three-electron bonding in **6d** and **7d**. If half of an electron hole is largely localized on each of these four atoms, one might expect each of them to be more positively charged than the other four chalcogen atoms. An NBO population analysis<sup>14</sup> does, in fact, find this to be the case; but the positive charges on the two different types of chalcogen atoms in **6d** and in **7d** differ by only 0.13, not 0.50. Clearly the electron-rich  $\pi$  orbitals of the eight-membered rings in the  ${}^3B_{3u}$  state of **6** and **7** donate more electron density into the  $\pi^*$  orbitals of those C=X bonds in which the chalcogen atom is involved in two-center, three-electron  $\sigma$  bonding.

There should also be a low-lying singlet state, corresponding to **6d** and **7d**, in which the electrons that have parallel spins in  ${}^3B_{3u}$  have antiparallel spins but remain localized on opposite sides of the molecules. Since  $e_{uy}$  and  $b_{1g}$  must be allowed to mix to obtain singly occupied, localized MOs, a broken symmetry (U)B3LYP calculation is necessary to find such an electronic state. Indeed, this type of calculation on **6d** and **7d** found each to have an electronic state with a pair of singly occupied orbitals containing electrons of opposite spin. This “singlet” state has essentially the same optimized geometry as the  ${}^3B_{3u}$  state and an energy that is lower than that of  ${}^3B_{3u}$  by 0.1 kcal/mol for **6d** and by 0.4 kcal/mol for **7d**.

**TABLE 2: Relative (U)B3LYP/6-31+G(d) Energies (kcal/mol) of the Low-Lying Singlet (a - c)<sup>b,c</sup> and Triplet<sup>d,e</sup> States of COT Derivatives **6** and **7** at  $D_{4h}$  Geometries<sup>a</sup>**

COT	a ( $^1A_{1g}$ ) <sup>b</sup>	b ( $^1A_{1g}$ ) <sup>b</sup>	c ( $^1A_{1g}$ ) <sup>c</sup>	$^3A_{1u}$ <sup>d</sup>	$^3A_{2u}$ <sup>d</sup>	$^3A_{2g}$ <sup>e</sup>	$^3E_u$ <sup>e,f</sup>
<b>6</b>	16.0 (16.6)	17.4 (18.8)	0 (0)	4.2 (5.2)	4.1 (4.6)	5.3 (5.5)	-1.9 (-1.8)
<b>7</b>	25.9 (23.4)	23.2 (21.0)	0 (0)	7.8 (6.8)	9.9 (8.8)	3.3 (2.0)	-5.8 (-7.4)

<sup>a</sup> Single-point energies, computed with the 6-311+G(2df) basis set at the (U)B3LYP/6-31+G(d) optimized geometries, are given in parentheses. <sup>b</sup> Both singlet states **a** and **b** have eight  $\pi$  electrons, but differ by whether the  $b_{1u}$  or  $b_{2u}$  COT  $\pi$  MO is doubly occupied. <sup>c</sup> Singlet state **c** has 10  $\pi$  electrons, with the  $b_{1g}$   $\sigma$  MO empty and the  $b_{1u}$  and  $b_{2u}$   $\pi$  MOs doubly occupied. <sup>d</sup> The  $^3A_{1u}$  and  $^3A_{2u}$  states each have nine  $\pi$  electrons, with one electron in the  $b_{1g}$   $\sigma$  MO. These two triplet states differ by whether the  $b_{1u}$  or  $b_{2u}$  COT  $\pi$  MO is singly occupied. <sup>e</sup> The  $^3A_{2g}$  and  $^3E_u$  states each have 10  $\pi$  electrons. In  $^3A_{2g}$ , the  $b_{1g}$   $\sigma$  MO is doubly occupied, and the unpaired electrons each occupy one of the degenerate pair of  $e_u$   $\sigma$  MOs, whereas in  $^3E_u$ , one of the unpaired electrons occupies the  $b_{1g}$   $\sigma$  MO, and the other occupies an  $e_u$   $\sigma$  MO. <sup>f</sup> Because the  $^3E_u$  state undergoes a first-order Jahn–Teller distortion,<sup>11</sup> its geometry cannot be fully optimized in  $D_{4h}$  symmetry. Therefore, the energies of the  $^3E_u$  states of **6** and **7** in Table 2 are based on calculations in which the molecules were constrained to maintain a geometry with  $D_{4h}$  symmetry.

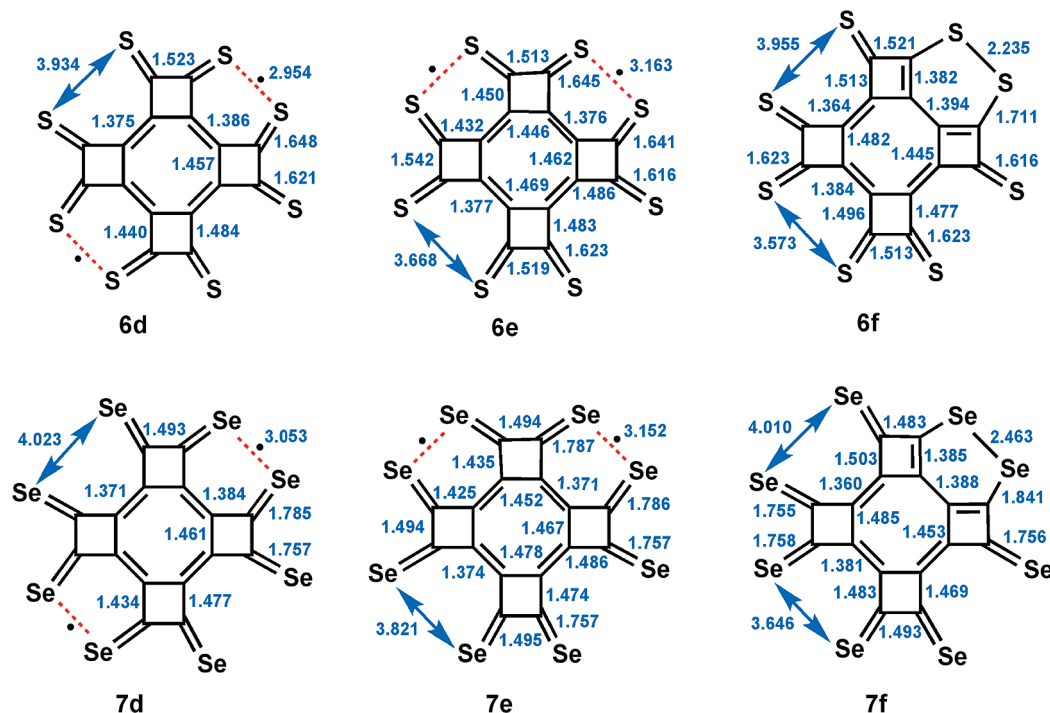


**Figure 4.** Bond lengths ( $\text{\AA}$ ) in the (U)B3LYP/6-31+G(d) optimized  $D_{2h}$  geometry of  $^3B_{3u}$  (**d**) and the optimized  $C_{2v}$  geometries of  $^3B_2$  (**e**) and  $^1A_1$  (**f**). As shown in the Supporting Information, the geometry of each of the two open-shell singlet states, is nearly the same as that of the triplet state, **d** or **e**, to which the open-shell singlet state corresponds. The dotted red lines in structures **d** and **e** indicate two-center, three-electron  $\sigma$  bonds between the chalcogen atoms, whereas in **f**, these two half-bonds are replaced by a full  $\sigma$  bond between two chalcogen atoms. In **d** and **e**, there are 10  $\pi$  electrons in the COT rings, in addition to the 16 electrons in the eight  $\pi$  bonds to the chalcogen atoms. In **f**, two of these eight  $\pi$  bonds are depicted as having been broken by becoming  $\pi$  lone pairs on the two chalcogen atoms that are  $\sigma$ -bonded to each other. However, the bond lengths in the six-membered rings of **6f** and **7f** clearly indicate that these  $\pi$  lone pairs are more delocalized than the resonance structures that are drawn for **6f** and **7f** would indicate.

However, a broken-symmetry, UB3LYP wave function with antiparallel spins for the electrons in the two singly occupied MOs is not really a singlet state, with  $S^2 = 0$ , but a 1:1 mixture of singlet and triplet states, with  $\langle S^2 \rangle \approx 1.0$ . Consequently, the energy of the pure ( $S^2 = 0$ ), open-shell singlet state that corresponds to the  $^3B_{3u}$  states of **6d** and **7d** can be estimated<sup>15</sup> to be, respectively, 0.2 and 0.8 kcal/mol lower than this triplet.

A proper description of a singlet that has a pair of electrons with antiparallel spins, each of which is localized in a different region of space, requires a two-configuration wave function.<sup>16</sup> For the singlet state of **6d** and **7d** that corresponds to the  $^3B_{3u}$  state, the singlet wave function has the form  $^1A_{1g} = (\dots e_{ux}^2 e_{uy}^2) - \dots e_{ux}^2 b_{1g}^2) / \sqrt{2}$ . This type of singlet wave function, like the wave function for  $^3B_{3u}$ , can be easily shown to place one electron in  $e_{uy} + b_{1g}$  and the other in  $e_{uy} - b_{1g}$ .<sup>16</sup>

Since a proper wave function for  $^1A_{1g}$  requires two configurations, we optimized the structures of **6d** and **7d** using

(2/2)CASSCF calculations for  $^1A_{1g}$  and ROHF calculations for the corresponding  $^3B_{3u}$  state. As with the UHF calculations, the (2/2)CASSCF geometry of the singlet and the ROHF geometry of the triplet were nearly identical. As predicted for a diradical in which the singly occupied MOs are disjoint (i.e., localized in different regions of space),<sup>16,17</sup> the (2/2)CASSCF energy of  $^1A_{1g}$  is nearly the same as the ROHF energy of  $^3B_{3u}$ , with the former 0.02 kcal/mol lower for both **6d** and **7d**.

Single-point CASPT2 calculations were carried out at the (2/2)CASSCF and ROHF optimized geometries. With inclusion of the effects of dynamic electron correlation<sup>18</sup> at the CASPT2 level, the  $^1A_{1g}$  state falls below the  $^3B_{3u}$  state by 1.2 kcal/mol for **6d** and 1.1 kcal/mol for **7d**.<sup>19</sup>

As already noted, the  $D_{2h}$  equilibrium geometry of the  $^3B_{3u}$  state of **6d** and **7d** comes from a  $b_{1g}$  Jahn–Teller distortion of the  $D_{4h}$  geometry of the  $^3E_u$  state. Group theory predicts that a  $b_{2g}$  vibration should also provide first-order Jahn–Teller energy



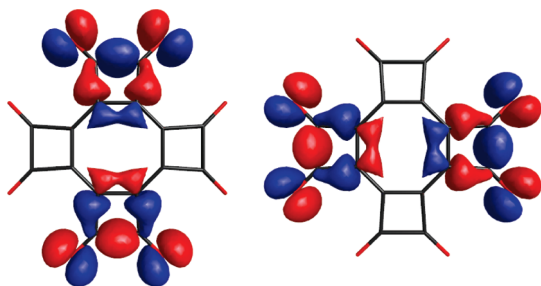


**Figure 5.** The  $e_u'$  MOs, which are the most useful MOs for analyzing the effect of a  $b_{2g}$  distortion in **6** and **7**.

lowering for the  ${}^3E_u$  state. However, unlike a  $b_{1g}$  vibration, which leads to a  $D_{2h}$  geometry that preserves the 2-fold axes and planes of symmetry that pass between the four-membered rings, a  $b_{2g}$  vibration leads to a  $D_{2h}$  geometry that preserves the 2-fold axes and planes of symmetry that pass through the four-membered rings. Upon this type of distortion, the  ${}^3E_u$  state in  $D_{4h}$  symmetry becomes a  ${}^3B_{2u}$  state in  $D_{2h}$  symmetry.

The energy lowering upon a  $b_{2g}$  distortion of  ${}^3E_u$  is only 2.0 kcal/mol for both **6** and **7**. The reason that the energy lowering is so much smaller for a  $b_{2g}$  than for a  $b_{1g}$  Jahn–Teller distortion is revealed by comparison of Figure 3 with Figure 5. The latter figure depicts another possible set of  $e_u$  MOs ( $e_u'$ ), which are the sum and difference of the  $e_u$  MOs in Figure 3.

The  $e_u'$  MOs are useful for discussing a  $b_{2g}$  distortion, which shortens the distances between the pairs of chalcogen atoms that are attached to four-membered rings on opposite sides of the COT ring and lengthens the distances between the pairs of chalcogen atoms that are attached to the other two four-membered rings. Inspection of Figure 5 shows that this type of distortion of the distances between pairs of chalcogen that are attached to the same four-membered ring causes one  $e_u'$  MO to go up in energy while the other  $e_u'$  MO goes down in energy.

Both Figures 3 and 5 show that the lone pair AOs on chalcogen atoms that are attached to the same four-membered ring are less favorably oriented for forming two-center, three-electron bonds than the lone pair AOs on chalcogen atoms that are attached to different four-membered rings. The  $b_{2g}$  distortion affects 1,4-interactions between chalcogens, whereas the  $b_{1g}$  distortion affects 1,6-interactions between chalcogens. Consequently, a  $b_{2g}$  distortion has a much smaller effect on lifting the degeneracy of the  $e_u'$  MOs in Figure 5 than a  $b_{1g}$  distortion has on lifting the degeneracy of the  $e_u$  MOs in Figure 3. This is the reason why a  $b_{2g}$  distortion is computed to provide a much smaller amount of Jahn–Teller stabilization for the  ${}^3E_u$  state than a  $b_{1g}$  distortion does.

We found that the optimized  $D_{2h}$  geometry that results from a  $b_{2g}$  Jahn–Teller distortion of  ${}^3E_u$  has two imaginary vibrational frequencies. Therefore, it is a mountain-top on the potential energy surface and, hence, of no chemical interest. The larger of these imaginary frequencies corresponds to a symmetry-breaking vibration that converts this  $D_{2h}$  geometry to the much lower energy  $D_{2h}$  geometry of **6d** and **7d**. The other imaginary frequency corresponds to a vibration that destroys just one plane and one axis of the  $D_{2h}$  symmetry operations and leads to the  $C_{2v}$  geometry of **6e** and **7e** in Figure 4.

The molecular distortion that leads to the optimized geometries of **6e** and **7e** in Figure 4 is driven in part by the mixing between the  $e_{uy}'$  MO that is doubly occupied in one component of the  ${}^3E_u$  wave function and the  $b_{1g}$  MO that is singly occupied. The resulting MO that is destabilized by this mixing remains singly occupied, and it corresponds to the  $a_1$  MO in Figure 6.

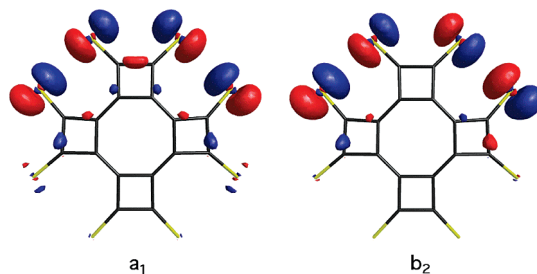


**Figure 6.** SOMOs of the  ${}^3B_2$  states of **6e** and **7e**. The sum and difference of these two MOs give localized, singly occupied MOs. Both the  $a_1$  and  $b_2$  SOMOs are antibonding between the pairs of chalcogens that participate in the two-center, three-electron bonds in **6e** and **7e**, but there are also doubly occupied  $a_1$  and  $b_2$  MOs that are bonding between these pairs of chalcogens.

The  $b_2$  MO in Figure 6 is the orbital that is destabilized by the mixing between the singly occupied  $e_{uy}'$  MO in Figure 5 and another doubly occupied MO. The two MOs in Figure 6 represent, respectively, the in-phase and out-of-phase combinations of the localized orbitals that are each singly occupied in the pair of two-center, three-electron bonds between chalcogen atoms in **6e** and **7e**.

As shown in Figure 4, **6d**, **6e**, **7d**, and **7e** contain two, two-center, three-electron bonds between pairs of chalcogen atoms. The electronic structures of **d** and **e** differ by the fact that in **d**, these two-center, three-electron bonds are formed between pairs of chalcogen atoms that are attached to two different pairs of four-membered rings, whereas in **e**, two of the chalcogen atoms that form these bonds are attached to the same four-membered ring.

One might imagine Coulombic repulsions between positively charged electron holes would make participation in two-center, three-electron bonds more difficult for two chalcogen atoms attached to the same four-membered ring than for two chalcogens attached to different four-membered rings. Indeed, the chalcogen atoms, attached to the same four-membered ring in **6e** and **7e** have, respectively, 0.17 and 0.08 less spin density and 0.07 and 0.05 less positive charge than the other two chalcogen atoms to which they are bonded. In addition, the two-center, three-electron bonds are longer by 0.2 Å in **6e** than in **6d** and by 0.1 Å in **7e** than in **7d**. As anticipated, Table 3 shows the energy of triplet **6e** is 7.4 kcal/mol higher than that of triplet **6d**, and the energy of triplet **7e** is 7.1 kcal/mol higher than that of triplet **7d**. The geometries and energies of the corresponding singlets differ by similar amounts.

Vibrational analyses found that both singlet and triplet states of **6e** have one imaginary frequency, corresponding to a vibration that connects **6e** to the two equivalent geometries of **6d**. Therefore, **6e** is the transition structure that connects the two, equivalent, **6d** energy minima on both the singlet and triplet potential energy surfaces.

In contrast, neither the singlet nor the triplet states of **7e** have any imaginary frequencies. Therefore, they are both energy minima. However, **7e** still presumably lies on the reaction path that connects the two equivalent **7d** energy minima on both the singlet and triplet potential energy surfaces. We have not made any effort to locate the transition structure that connects **7d** to **7e** on either the singlet or triplet energy surfaces.

It was also possible to optimize the geometry of singlet states **6f** and **7f**, in which the pairs of two-center, three-electron bonds between sulfur atoms in **6d** and **6e** and between pairs of selenium atoms in **7d** and **7e** are each replaced by one full  $\sigma$  bond. The B3LYP optimized geometries of **6f** and **7f** are shown in Figure 4, and their energies are given in Table 3.

**TABLE 3: Relative Single-Point (U)B3LYP/6-311+G(2df) Energies of the Low-Lying Electronic States of COT Derivatives 6 and 7, Computed at the (U)B3LYP/6-31+G(d) Optimized Geometries Shown in Figures 4 and 7**

COT	c	d ( $^3B_{3u}$ )	d ( $^1A_{1g}$ )	e ( $^3B_2$ )	e ( $^1A_1$ )	f ( $^1A_1$ )	g	h	i	TS <sub>c-g</sub>
6	0	-11.8	-11.9	-4.4	-5.2	-4.4	-3.7	-15.6	-33.0	9.2
7	0	-21.3	-21.7	-14.2	-14.3	-13.0	8.0	-13.2	-37.7	8.8

It is noteworthy that, despite the full  $\sigma$  bond between chalcogen atoms in **6f** and **7f**, each of these singlets is higher in energy than the singlet state of both of its isomers (**6d** and **6e** and **7d** and **7e**) that contain two two-center, three-electron bonds between chalcogens. Two such partial bonds, each formed by two electrons in a bonding MO and one electron in an antibonding MO, might be expected to be weaker than one full  $\sigma$  bond, but the relative energies in Table 3 indicate that this is not the case in **6** and **7**.

Formation of the S–S bond in **6f** and the Se–Se bond in **7f** is made possible by the existence of a one-electron hole in the  $\sigma$  lone pairs on each of the two chalcogen atoms that are singly bonded to each other. Therefore, there is likely to be a large amount of Coulombic repulsion between the positive charges on these two atoms, and this repulsion should tend to destabilize **6f** relative to **6d** and **6e**, and **7f** relative to **7d** and **7e**.

In fact, an NBO analysis finds that the charge on each of the chalcogen atoms that are bonded to each other is 0.35 in **6f** and 0.42 in **7f**. These positive charges are significantly larger than those on the other three types of sulfur atoms (0.18, 0.14 and 0.18) in **6f** and on the other three types of selenium atoms (0.24, 0.22, and 0.26) in **7f**.

The positive charges on the chalcogen atoms that are bonded to each other are partially ameliorated by donation of  $\pi$  electrons from the eight-membered ring into the antibonding C=X  $\pi^*$  orbitals. In fact, the resonance structures shown for **6f** and **7f** in Figure 4 are drawn as though this electron donation is so

complete that it leads to the breaking of the C=X  $\pi$  bonds to the chalcogen atoms that are bonded to each other, leaving a lone pair of  $\pi$  electrons on each chalcogen atom.

However, the resonance structures for **6f** and **7f** in Figure 4 overemphasize the localization of the  $\pi$  lone pairs on these two chalcogens, since the lone pairs can be donated into the adjacent C=C  $\pi$  bonds. Some of the effects of this electron delocalization can be seen in Figure 4 in the anomalous C–X and C–C bond lengths in the six-membered rings that contain the chalcogen atoms that are bonded to each other.

As discussed above, another effect of lone pair donation into the  $\pi$  bonds is the large size of NBO partial positive charges on each of these pairs of chalcogen atoms (0.35 in **6f** and 0.42 in **7f**). As already noted, we believe these positive charges destabilize **6f** relative to **6d** and **6e**, and **7f** relative to **7d** and **7e**.

**Isomers of 6 and 7 with One Less Four-Membered Ring.** Our previous B3LYP calculations found that **1c** breaks symmetry to undergo a nearly barrierless and highly exothermic opening of one four-membered ring, to form bis-ketene **2**, which also has 10  $\pi$  electrons.<sup>1</sup> To investigate whether such a reaction also occurs in **6c** and **7c**, the sulfur and selenium analogs of **1**, we optimized the geometries of the chalcogen analogs of bis-ketene **2**, in which the O atoms in **2** are replaced by S and Se atoms.

Our calculations found that, unlike the case in the ring cleavage reaction of **1c** to bis-ketene **2**, the optimized  $C_{2v}$

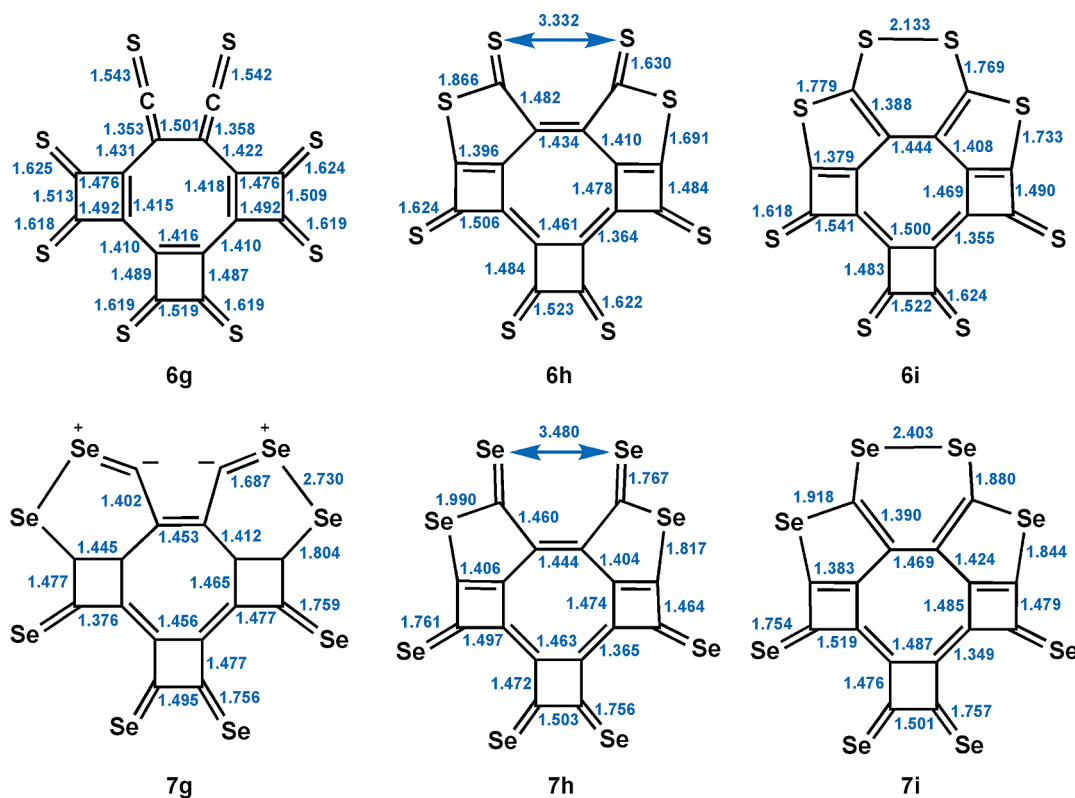


**Figure 7.** Bond lengths (Å) in the (U)B3LYP/6-31+G(d) optimized geometries of **6g**–**i** and **7g**–**i**. As indicated by the bond lengths, the bonding is much less localized than is suggested by the single resonance structure that is drawn for each of these molecules.

geometry of bis-thioketene **6g** is actually higher in energy than **6c** by 0.6 kcal/mol. However, the  $C_{2v}$  geometry of **6g** has three imaginary frequencies, and the fully optimized,  $C_1$  geometry of **6g**, which is shown in Figure 7, is lower in energy than **6c** by 3.7 kcal/mol but higher in energy than singlet diradical **6d** by 8.2 kcal/mol (Table 3). The transition structure that connects **6c** to **6g** is 9.2 kcal/mol higher than **6c**.

Once formed, **6g** can undergo almost barrierless, stepwise, bis-thiolactonization to form **6h**. The geometries and energies of the two transition states and the intermediate connecting **6g** to **6h** are given in the Supporting Information. As shown in Table 3, formation of **6h** from **6g** is calculated to be exothermic by 12.6 kcal/mol, so **6h** is predicted to be slightly lower in energy than singlet diradical **6d**.

Electrocyclization of **6h** to **6i** is also calculated to be energetically favorable, and the transition structure for this reaction is computed to be only 1.4 kcal/mol higher in energy than **6h**. As shown in Table 3, the ring closure that converts **6h** to **6i** is calculated to be exothermic by 17.4 kcal/mol. Therefore, disulfide **6i** is predicted to be considerably lower in energy than singlet diradical **6d**.

We were unable to locate a minimum corresponding to the selenium analog of bis-thioketene **6g**. Attempts led to the formation of the two Se–Se single bonds in **7g**, which is calculated to be  $\sim 8.0$  kcal/mol higher in energy than **7c**.

As shown in Table 3, bis-selenolactone **7h** is computed to be 13.2 kcal/mol lower in energy than **7c**, but 8.5 kcal/mol higher in energy than singlet diradical **7d**. However, Se–Se bond formation in the cyclization of **7h** to **7i** is computed to be about 10 kcal/mol more exothermic than S–S bond formation in the cyclization of **6h** to **6i**. The large exothermicity of the cyclization of **7h** to **7i** makes the energy of **7i** about 16.0 kcal/mol lower than that of singlet diradical **7d**.

Thus, our calculations indicate that singlet diradicals **6d** and **7d** are not the lowest energy isomers on either of the  $C_{16}X_8$  ( $X = S, Se$ ) potential energy surfaces. However, if formed, at low temperatures, **6d** and **7d** might be expected to have some kinetic stability. Conversion of **6d** to **6i** and **7d** to **7i** would presumably pass through **6c** and **7c**, respectively, as the intermediates in the ring-opening reactions that afford **6g** and **7g**. The transition structures for the opening of a four-membered ring in **6c** and **7c** are calculated to be, respectively, 21.1 and 30.5 kcal/mol higher in energy than singlet diradicals **6d** and **7d**. These are, presumably, the heights of the barriers that separate **6d** from **6i**, and **7d** from **7i**. Consequently, if formed at low temperature, diradical **6d** is predicted to be kinetically stable toward rearrangement to **6i**, whereas even at room temperature, diradical **7d** should be kinetically stable toward rearrangement to **7i**.

## Conclusions

Our B3LYP calculations predict that in tetrakis-annulated cyclooctatetraenes **6** and **7**, electronic states with an aromatic defect of 10  $\pi$  electrons in the eight-membered ring are lower in energy than electronic states with 8 or 9  $\pi$  electrons. Model calculations on **3**–**5** show that transfer of a pair of electrons from a high-energy  $\sigma$  MO to a low-energy  $\pi$  MO is made more favorable in **6** and **7** than in **1** by the lower  $\sigma$  IP and higher  $\pi$  EA when oxygen in 1,2-cyclobutanedione is replaced by sulfur or selenium.

Our calculations on **6** and **7** at  $D_{4h}$  geometries find that the  $10-\pi$   ${}^3E_u$  state, formed by  $n \rightarrow \pi$  excitation of one electron each from the  $b_{1g}$  and  $e_u$   $\sigma$  MOs, is lower in energy than the  $10-\pi$   ${}^1A_{1g}$  state, formed by  $n \rightarrow \pi$  excitation of both electrons from the  $1b_{1g}$  HOMO. The  ${}^3E_u$  state is subject to  $b_{1g}$  and  $b_{2g}$  first-

order Jahn–Teller distortions. The former is computed to be the more energetically favorable and leads to a triplet diradical with a  $D_{2h}$  geometry, containing two-center, three-electron bonds between two pairs of sulfur atoms in **6d** and selenium atoms in **7d**. Because the two, singly occupied MOs in each triplet can be localized to different regions of space, an open-shell singlet, with one electron in each of these disjoint, localized MOs is calculated to be close in energy to and actually slightly lower than the corresponding triplet state.

Additional calculations find that **6i** is lower in energy than **6d** and that **7i** is lower in energy than **7d**. However, formation of **6i** and **7i** from **6d** and **7d**, respectively, would presumably proceed by opening of one of the four-membered rings in **6c** and **7c**. If this is, indeed, the lowest energy pathway connecting **6d** to **6i** and **7d** to **7i**, barriers of 21.1 and 30.5 kcal/mol, respectively, are predicted to separate singlet **6d** from **6i** and singlet **7d** from **7i**. Therefore, at low temperatures, singlet diradical **6d** and, even more so, singlet diradical **7d** might prove to be kinetically stable toward rearrangement to their more thermodynamically stable isomers, **6i** and **7i**.

Our calculations find that **6d** and **7d**, in which the  $\pi$  MOs of the eight-membered rings contain 10  $\pi$  electrons, are considerably lower in energy than both of the COT bond-shift isomers in which the  $\pi$  MOs of the eight-membered ring contain 8  $\pi$  electrons. Thus, if diradicals **6d** and **7d** can be prepared and isolated, we predict that they will prove to be the first derivatives of COT in which excitation of two electrons from  $\sigma$  to  $\pi$  MOs is found to be thermodynamically favorable.

**Acknowledgment.** We thank the National Science and Robert A. Welch Foundations for support of this research. Some of the results reported here were obtained on computers purchased with funds provided by the National Science Foundation under Grant CHE-0741936.

**Supporting Information Available:** The optimized (U)B3LYP/6-31+G(d) geometries and energies for all the molecules and transition structures in Tables 1–3 and a complete list of authors for ref 7 (55 pages). This information is available free of charge via the Internet at <http://pubs.acs.org>.

## References and Notes

- (1) Zhou, X.; Hrovat, D. A.; Borden, W. T. *Org. Lett.* **2008**, *10*, 893.
- (2) (a) Similarly, Gleiter and his coworkers have found that low-lying electronic states of cyclobutanetetraene are formed by excitations of one or two electrons from the  $b_{1g}$   $\sigma$  HOMO into the  $a_2$   $\pi^*$  LUMO. Gleiter, R.; Hyla-Kryspin, I.; Pfeifer, K.-H. *J. Org. Chem.* **1995**, *60*, 5878. Subsequent calculations have predicted that the ground state of cyclobutanetetraene is actually the triplet with nine  $\pi$  electrons. (b) Jiao, H.; Frapper, G.; Halet, J.-F.; Saillard, J.-Y. *J. Phys. Chem A* **2001**, *105*, 5945. (c) Zhou, X.; Hrovat, D. A.; Gleiter, R.; Borden, W. T. *Mol. Phys.* **2009**, *107*, 863. (d) Zhou, X.; Hrovat, D. A.; Borden, W. T. *J. Phys. Chem A* **2009**, *113*, 1304.
- (3) Becke, A. D. *J. Chem. Phys.* **1993**, *98*, 5648.
- (4) Lee, C.; Yang, W.; Parr, R. G. *Phys. Rev. B* **1998**, *37*, 785.
- (5) Francl, M. M.; Pietro, W. J.; Hehre, W. J.; Binkley, J. S.; Gordon, M. S.; DeFrees, D. J.; Pople, J. A. *J. Chem. Phys.* **1982**, *77*, 3654.
- (6) Krishnan, R.; Binkley, J. S.; Seeger, R.; Pople, J. A. *J. Chem. Phys.* **1980**, *72*, 650.
- (7) Frisch, M. J., *Gaussian 03, Revision D.02*; Gaussian, Inc.: Wallingford, CT, 2004.
- (8) (a) Anderson, K.; Malmqvist, R. A.; Roos, B. O. *J. Chem. Phys.* **1992**, *96*, 1218. (b) Anderson, K.; Malmqvist, R. A.; Roos, B. O.; Sadlej, A. J.; Wolinski, K. *J. Chem. Phys.* **1990**, *94*, 5483.
- (9) Hariharan, P. C.; Pople, J. A. *Theor. Chim. Acta* **1973**, *28*, 213.
- (10) MOLCAS Version 6.4 Karlström, G.; Lindh, R.; Malmqvist, P.-Å.; Roos, B. O.; Ryde, U.; Veryazov, V.; Widmark, P.-O.; Cossi, M.; Schimmelpfennig, B.; Neogrady, P.; Seijo, L. *Comput. Mater. Sci.* **2003**, *28*, 222.
- (11) Jahn, H. A.; Teller, E. *Proc. R. Soc. London, Ser. A* **1937**, *161*, 220.

(12) Many-electron wavefunctions are invariant to taking orthonormal linear combinations of MOs that are occupied by electrons of the same spin.

(13) For a review, see: Asmus K.-D. In *Sulfur-Centered Reactive Intermediates in Chemistry and Biology*; Chatgililoglu, C., Asmus, K.-D., Eds; Plenum Press: New York, 1990; pp 155–172.

(14) Reed, A. E.; Weinstock, R. B.; Weinhold, F. *J. Chem. Phys.* **1985**, *83*, 735.

(15) Yamaguchi, K.; Jensen, F.; Dorigo, A.; Houk, K. N. *Chem. Phys. Lett.* **1988**, *149*, 537.

(16) (a) For reviews, see: Borden, W. T. In *Diradicals*; Borden, W. T., Ed.; Wiley-Interscience: New York, 1982; pp 1–72. (b) Borden, W. T. In *Encyclopedia of Computational Chemistry*; Schleyer, P. von R., Allinger, N. L., Clark, T., Gasteiger, J., Kollman, P. A., Schaefer, H. F., III, Schreiner, P. R., Eds.; Wiley: Chichester, UK, 1998; pp 708–722.

(17) Borden, W. T.; Davidson, E. R. *J. Am. Chem. Soc.* **1977**, *99*–4587.

(18) Borden, W. T.; Davidson, E. R. *Acc. Chem. Res.* **1996**, *29*, 87.

(19) The  ${}^1A_{1g}$  state distorts from  $D_{4h}$  symmetry to  $D_{2h}$  symmetry under the influence of a second-order Jahn–Teller effect.<sup>16</sup> At  $D_{4h}$  geometry, the lowest  ${}^1A_{1g}$  wave function consists of the lowest energy configuration,  ${}^1A_{1g} = (l\dots e_{ux}^2e_{uy}^2)$ , with an admixture of the configurations  $(l\dots e_{ux}^2b_{1g}^2) + l\dots e_{uy}^2b_{1g}^2)/\sqrt{2}$ . This pair of excited configurations provides correlation for the pairs of electrons that occupy the same MO in the configuration of lowest energy. On a molecular distortion of  $b_{1g}$  symmetry, these three configurations can mix with the low-lying  ${}^1B_{1g}$  excited state,  $(l\dots e_{ux}^2b_{1g}^2) - l\dots e_{uy}^2b_{1g}^2)/\sqrt{2}$ . The mixing occurs so that the second term in the resulting  $D_{2h}$  wave function is either  $l\dots e_{ux}^2b_{1g}^2$  or  $l\dots e_{uy}^2b_{1g}^2$ , depending on which degenerate  $\sigma$  MO is stabilized by the distortion.

JP911705Y